

# Nontrivial multi-product commutation relation for reducing $T$ -count in sequential Pauli-based computation

Yusei Mori,<sup>1,\*</sup> Hideaki Hakoshima,<sup>1,2,†</sup> and Keisuke Fujii<sup>1,2,3,‡</sup>

<sup>1</sup>*Graduate School of Engineering Science, The University of Osaka,  
1-3 Machikaneyama, Toyonaka, Osaka 560-8531, Japan*

<sup>2</sup>*Center for Quantum Information and Quantum Biology,*

*The University of Osaka, 1-2 Machikaneyama, Toyonaka, Osaka 560-0043, Japan*

<sup>3</sup>*RIKEN Center for Quantum Computing, 2-1 Hirosawa, Wako, Saitama 351-0198, Japan*

Quantum compilers that reduce the number of  $T$  gates are essential for minimizing the overhead of fault-tolerant quantum computation. To achieve effective  $T$ -count reduction, it is necessary to identify equivalent circuit transformation rules that are not yet utilized in existing tools. In this paper, we rewrite any given Clifford+ $T$  circuit using a Clifford block followed by a sequential Pauli-based computation, and introduce a nontrivial and ancilla-free equivalent transformation rule, the multi-product commutation relation (MCR). This rule constructs gate sequences based on specific commutation properties among multi-Pauli operators, yielding seemingly non-commutative instances that can be commuted. To evaluate whether existing compilers account for this commutation rule, we create a benchmark circuit dataset using quantum circuit unoptimization. This technique intentionally adds redundancy to the circuit while keeping its equivalence. By leveraging the known structure of the original circuit before unoptimization, this method enables a quantitative evaluation of compiler performance by measuring how closely the optimized circuit matches the original one. Our numerical experiments reveal that the transformation rule based on MCR is not yet incorporated into current compilers. This finding suggests an untapped potential for further  $T$ -count reduction by integrating MCR-aware transformations, paving the way for improvements in quantum compilers.

## I. INTRODUCTION

Quantum computing has the potential to outperform classical computation in specific tasks such as factorization [1], unstructured database search [2], and simulation of quantum many-body systems [3, 4]. While these algorithms promise significant theoretical speedups, their practical implementation requires expressing them as quantum circuits that meet the constraints of physical quantum hardware. The ongoing increase in the number of physical qubits and the improvement of gate fidelity bring the construction of fault-tolerant quantum computers (FTQC) closer to practicality [5, 6]. In this emerging landscape, addressing resource constraints becomes increasingly essential, particularly the high implementation cost of specific gates in FTQC.

In FTQC architectures, the Clifford+ $T$  gate set stands out as a leading candidate for universal quantum computation [7] due to its compatibility with quantum error correction. Clifford gates are commonly implemented using transversal operations, which are relatively low-cost. However, non-Clifford gates such as the  $T$  gate are substantially more expensive to implement fault-tolerantly, primarily due to the need for magic state distillation [8]. Therefore, reducing the number of  $T$  gates in quantum circuits, a process known as  $T$ -count optimization, has

emerged as a key challenge for the efficient implementation of quantum algorithms on FTQC.

To enable efficient  $T$ -count reduction, quantum compilers form an essential component of the quantum computing stack, serving as an intermediate layer between high-level descriptions of quantum algorithms and low-level, hardware-specific implementations [9–11]. This design is derived from the role of classical compilers, which translate high-level programming languages into machine-level instructions [12]. Quantum compilers perform not only gate count reduction in quantum circuits but also a range of tasks, including gate decomposition [13–15] and qubit mapping for hardware compatibility [16–19].

From the perspective of circuit optimization, a common strategy is to rewrite a quantum circuit into an intermediate representation (IR), apply optimization rules specialized for that representation, and translate it back into a quantum circuit. Several IRs have been proposed for  $T$ -count reduction. The first is the  $ZX$ -calculus, a graphical framework which expresses quantum circuits as diagrams and simplifies them using rewrite rules such as spider fusion [20, 21] and phase gadgetization [22]. The latter technique enables specific nonlocal optimizations when the involved gadgets can be propagated through the  $ZX$ -diagram. Nonetheless, the effectiveness of these techniques remains limited due to the presence of non-commuting gates within the circuit, such as internal Hadamard gates, which restrict simplification to local transformations. Another well-known approach is the *phase-polynomial*, an algebraic representation which encodes CNOT+ $T$  circuits as linear Boolean functions and

---

\* [u839526i@ecs.osaka-u.ac.jp](mailto:u839526i@ecs.osaka-u.ac.jp)

† [hakoshima.hideaki.es@osaka-u.ac.jp](mailto:hakoshima.hideaki.es@osaka-u.ac.jp)

‡ [fujii.keisuke.es@osaka-u.ac.jp](mailto:fujii.keisuke.es@osaka-u.ac.jp)

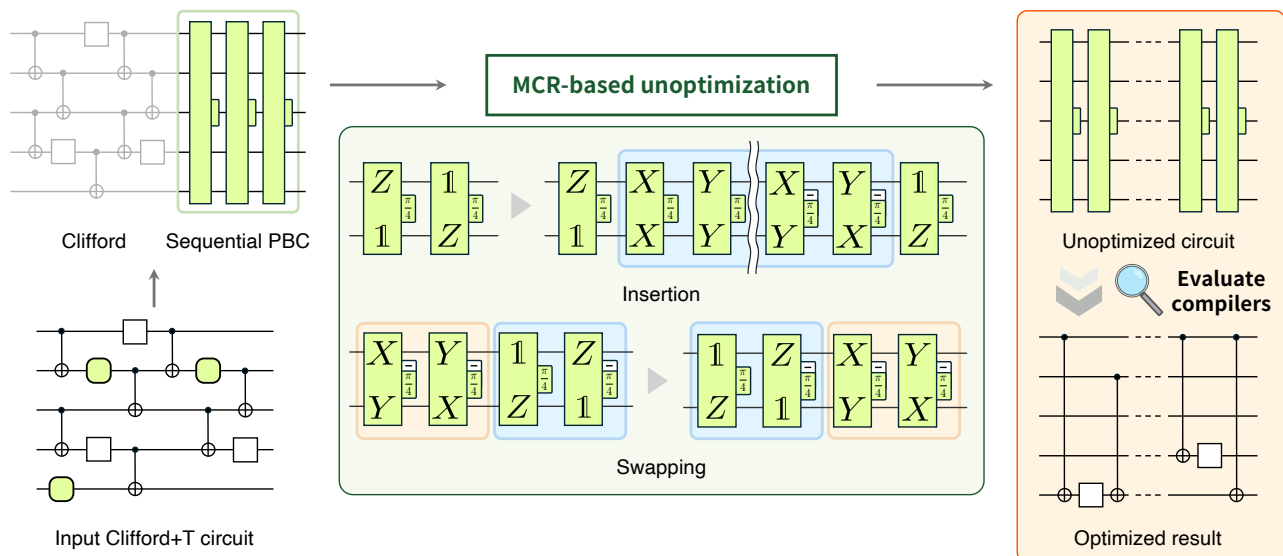


FIG. 1. An overview of the quantum compiler benchmarking procedure for Clifford+ $T$  circuits using MCR-based unoptimization. Starting from an input Clifford+ $T$  circuit, we first reorder all  $T$  gates with adjacent Clifford gates to separate the Clifford part and yield a sequential Pauli-based computation. Then, we apply the multi-product commutation relation (MCR) to the non-Clifford block, intentionally introducing redundant gates and yielding an *unoptimized* circuit that is functionally equivalent but has a larger  $T$ -count. A target quantum compiler then attempts to compress this circuit and produces an optimized output, whose  $T$ -count is compared with that of the original circuit. If the compiler fails to recover to the original optimal  $T$ -count, analyzing the gap makes it possible to improve the compiler’s performance.

enables algorithmic optimization methods [23–25]. Extensions of this technique to Clifford+ $T$  circuits have been proposed, a process known as *Hadamard gadgetization* [26–28]. Though this approach enables representing the entire circuit within the CNOT+ $T$  framework, it inevitably introduces additional ancilla qubits, typically requiring one ancilla qubit per Hadamard gate. In the context of FTQC, these ancilla qubits must be implemented as fault-tolerant logical qubits, further increasing the resource requirements.

As an approach that can potentially overcome the limitations of the methods mentioned above, the *sequential Pauli-based Computation (sequential PBC)* expresses a Clifford+ $T$  circuit as a sequence of  $\pm\pi/4$  multi-Pauli rotation gates obtained by rearranging all Clifford gates to the beginning of the circuit while keeping the overall equivalence [29]. Notably, originally proposed as a framework for performing lattice surgery in surface codes, sequential PBC has been shown to be not only effective for reducing the  $T$ -count but also well-suited for optimizations targeting the instruction sets of FTQC [30, 31]. In the context of  $T$ -count reduction, sequential PBC has demonstrated performance comparable to other IRs, as exemplified by the compiler, TMerge [32, 33]. However, its optimization rules are currently restricted to mutually commuting Pauli rotations and thus cannot be directly applied to non-commuting cases.

In this paper, we introduce a nontrivial and ancilla-free circuit transformation rule for quantum circuits, the *multi-product commutation relation (MCR)*, which is de-

efined as a sequential PBC format. MCR constructs a sequence consisting of multi-Pauli rotation gates that anticommute with each other but commute collectively. To show that MCR is a nontrivial equivalent transformation, we need to demonstrate that  $T$ -count optimization compilers are challenging in optimizing quantum circuits made redundant by this transformation. We employ MCR in an algorithm called *quantum circuit unoptimization* [34], which intentionally introduces redundancy to the circuit while keeping its equivalence. The schematic workflow of the quantum circuit unoptimization algorithm is shown in Fig. 1. Using this process, we can guarantee the optimal  $T$ -count from the original quantum circuit, allowing us to quantitatively analyze the performance of compilers in optimizing redundant  $T$  gates. Using the unoptimized circuits as benchmarks, where redundant  $T$  gates are introduced by MCR, we evaluate the performance of four types of  $T$  gate optimization compilers, specifically those based on the ZX-calculus, phase-polynomial, and sequential PBC representations. Our results show that these state-of-the-art compilers, despite their different optimization frameworks, fail to reduce the  $T$ -count comparable to that of the original circuit. This finding demonstrates that MCR is a nontrivial equivalent transformation not currently incorporated in compilers, suggesting the potential for integrating MCR-based transformations into future compilation passes, leading to more globally aware  $T$ -count reduction.

The structure of this paper is as follows. Sec. II provides the preliminary, introducing the Pauli and Clif-

ford groups as well as a set of rotation axes used to define multi-Pauli rotation gates. Also, we describe a method for separating the Clifford+ $T$  circuit into a sequence only composed of Clifford gates and a sequential PBC derived from  $T$  gates. In Sec. III, we define and formulate a nontrivial gate commutation rule, MCR, which enables transformations not evident from adjacent gate commutativity alone. We also provide a condition for constructing MCR. Sec. IV verifies the non-obviousness of MCR through compiler benchmarks based on quantum circuit unoptimization. We also explain the experimental setup and present the numerical results in detail. Finally, Sec. V concludes our study and outlines potential directions for future research.

## II. PRELIMINARY

### A. Multi-Pauli rotations

We begin with defining the  $n$ -qubit *Pauli group*  $\mathcal{P}_n$  as the group generated by  $n$ -fold tensor products of the single-qubit Pauli operators  $\{I, X, Y, Z\}$ , multiplied by coefficients from the set  $\{\pm 1, \pm i\}$ :

$$\mathcal{P}_n = \{\pm 1, \pm i\} \times \{I, X, Y, Z\}^{\otimes n}. \quad (1)$$

We also use the *Clifford group*  $\mathcal{C}_n$  as the set of unitary operators that map every element of  $\mathcal{P}_n$  to another element of  $\mathcal{P}_n$  under conjugation:

$$\mathcal{C}_n = \{C \mid CPC^\dagger \in \mathcal{P}_n, \forall P \in \mathcal{P}_n\}. \quad (2)$$

Representative elements of the Clifford group include the Hadamard ( $H$ ), phase ( $S$ ), and CNOT gates:

$$H = \frac{1}{\sqrt{2}} \begin{pmatrix} 1 & 1 \\ 1 & -1 \end{pmatrix}, \quad (3)$$

$$S = \begin{pmatrix} 1 & 0 \\ 0 & i \end{pmatrix}, \quad (4)$$

$$\text{CNOT} = \begin{pmatrix} 1 & 0 & 0 & 0 \\ 0 & 1 & 0 & 0 \\ 0 & 0 & 0 & 1 \\ 0 & 0 & 1 & 0 \end{pmatrix}. \quad (5)$$

Clifford gates alone are not *universal*, meaning that they cannot implement arbitrary unitary operations on quantum circuits [7]. To achieve universality, it is necessary to include non-Clifford gates, and a widely used example is the  $T$  gate:

$$T = \begin{pmatrix} 1 & 0 \\ 0 & e^{i\frac{\pi}{4}} \end{pmatrix}. \quad (6)$$

Both the Clifford and  $T$  gates can be expressed as products of *multi-Pauli rotation gates*. They are unitary operations of the form

$$R_P(\theta) = e^{-i\theta P/2} = \cos\left(\frac{\theta}{2}\right)I^{\otimes n} - i \sin\left(\frac{\theta}{2}\right)P, \quad (7)$$

where  $\theta \in (-\pi, \pi]$  is the *rotation angle*, and  $P$  is the *rotation axis*, chosen from a set of rotation axes  $\mathcal{P}_n^* \subset \mathcal{P}_n$ , defined as

$$\mathcal{P}_n^* := \{\pm 1\} \times \{I, X, Y, Z\}^{\otimes n} \setminus \{\pm I^{\otimes n}\}. \quad (8)$$

This set consists of Hermitian Pauli operators excluding the identity  $\pm I^{\otimes n}$ . All Clifford operators can be rewritten as sequences of multi-Pauli rotations with angles of the form  $k\pi/2$  for some integer  $k$ . For example, the Hadamard gate admits the decomposition  $\exp(i\pi/2)R_Z(\pi/2)R_X(\pi/2)R_Z(\pi/2)$ , and similar expressions exist for  $S$  and CNOT. On the other hand,  $T$  gate is expressed as a  $\pi/4$  multi-Pauli rotation gate  $\exp(i\pi/8)R_Z(\pi/4)$ . We sometimes denote the multi-qubit Pauli rotation gates with identity operators ( $I$ ) appended as needed to ensure consistency with the total number of qubits in the circuit, e.g.,  $R_{IXII}(\pi/4) = IR_X(\pi/4)II$ .

In this paper, we consider a Clifford+ $T$  circuit that contains many multi-Pauli rotation gates. To clearly illustrate their structure, we adopt a diagrammatic representation that explicitly shows the rotation axis and angle for each gate [30]. For each qubit, the rotation axis ( $\mathbb{1}, X, Y, Z$ ) is written inside a box, and the rotation angle is placed outside. Here,  $\mathbb{1}$  denotes the identity operator  $I$ . Gates with a rotation angle of  $\pm\pi/4$  (i.e., non-Clifford gates) are colored green, while those with a phase of  $k\pi/2$  (i.e., Clifford gates) are colored orange. For example,  $T$  gate,  $S^\dagger$  gate, and  $R_{XIZ}(\pi/4)$  are visualized according to this rule as shown in Fig. 2.

Each multi-Pauli rotation gate  $R_P(\theta)$  can be decomposed into a gate sequence consisting of a single-qubit  $Z$ -rotation gate and Clifford gates from the set  $\{\text{CNOT}, H, S, S^\dagger\}$ . This decomposition can be achieved in two steps. First, any rotation of the form  $R_{Z\dots Z}(\theta)$  is reduced to a single-qubit  $Z$ -rotation acting on one of the qubits, combined with CNOT gates. Fig. 3 illustrates an example of the transformation of the four-qubit gate  $R_{ZZZZ}(\theta)$ . Next, to handle a general Pauli axis  $P \in \mathcal{P}_n^*$ , we apply local Clifford gates before and after the  $Z$ -rotation to convert into a rotation around  $P$ . For example, to change the rotation axis from  $Z$  to  $X$ , we apply Hadamard gates before and after. To convert it into  $Y$ , we use  $\{S^\dagger, H\}$  before and  $\{H, S\}$  after. Using these steps, a gate such as  $R_{YXZ}(\theta)$  can be equivalently transformed as shown in Fig. 4.

### B. Sequential PBC

We separate a given Clifford+ $T$  circuit into Clifford gates and non-Clifford multi-Pauli rotations as introduced in Sec. II A. The order of operation between a Clifford gate and a  $T$  gate can generally be exchanged by replacing the  $T$  gate with a modified gate  $\tilde{T}$  defined

$$\begin{aligned}
 T &= \boxed{Z}_{\pi/4} \\
 S^\dagger &= \boxed{Z}_{-\pi/2} \\
 R_{XIZ}\left(\frac{\pi}{4}\right) &= \boxed{X}_{\pi/4} \\
 &\quad \boxed{1}_{\pi/4} \\
 &\quad \boxed{Z}
 \end{aligned}$$

FIG. 2. Representation of quantum gates used in this paper. The rotation axis is indicated inside each box, and the rotation angle is shown outside. Gates with rotation angles of  $\pm\pi/4$  (non-Clifford) are colored green, while those with  $k\pi/2$  ( $k \in \mathbb{Z}$ , Clifford) are colored orange.

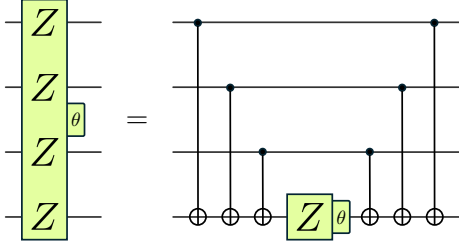


FIG. 3. Decomposition of the multi-Pauli rotation gate  $R_{ZZZZ}(\theta)$ . The gate applies a rotation about the tensor product of four Pauli-Z operators, and is decomposed into a standard circuit using a sequence of CNOT gates and a single-qubit Z-rotation.

as

$$\begin{aligned}
 \tilde{T} &= CTC^\dagger \\
 &= e^{i\frac{\pi}{8}} CR_Z\left(\frac{\pi}{4}\right)C^\dagger \\
 &= e^{i\frac{\pi}{8}} R_{CZC^\dagger}\left(\frac{\pi}{4}\right).
 \end{aligned} \tag{9}$$

By repeatedly applying this operation to adjacent Clifford gates, any  $T$  gate can be propagated to the right end of the circuit. Fig. 5 illustrates an example of  $T$  propagation. Using Eq. (9), this operation yields a new rotation axis  $-XYX$  in the end.

By repeating this procedure for all  $T$  gates in a Clifford+ $T$  circuit, we can express the circuit as the product of Clifford gates followed by the *sequential Pauli-based Computation (sequential PBC)* without loss of generality [29]. That is, given a Clifford+ $T$  circuit  $U = e^{i\phi} C'_0 T^{\otimes l_1} C'_1 T^{\otimes l_2} C'_2 \dots C'_{k-1} T^{\otimes l_k} C'_k$ , where  $\phi$  is a global phase, and  $T^{\otimes l_i}$  ( $i = 1, \dots, k$ ) denotes the  $T$  gates acting on  $l_i$  qubits between the  $(i-1)$ -th and  $i$ -th Clifford sequences, we can convert it into the following form

$$U = e^{i\phi} \left\{ \prod_{i=1}^k R_{P_i}\left(\frac{\pi}{4}\right) \right\} C_k. \tag{10}$$

In this paper, we focus primarily on the non-Clifford part, as it determines the  $T$ -count of the circuit. Note that the above procedure can also be applied to Clifford+ $R_Z$  circuits, i.e., circuits that consist of Clifford gates and

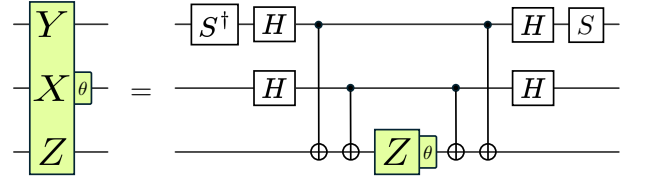


FIG. 4. Decomposition of the three-qubit rotation gate  $R_{YXZ}(\theta)$ . The gate implements a rotation about the tensor product of  $Y$ ,  $X$ , and  $Z$ , and is decomposed into a standard circuit using local Clifford gates and a single  $Z$ -rotation.

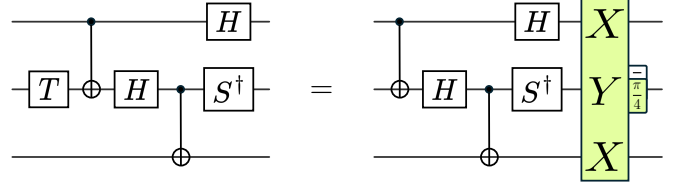


FIG. 5. Transformation of a circuit segment containing one  $T$  gate surrounded by Clifford gates. In the transformed circuit, the Clifford gates remain unchanged, and a multi-Pauli rotation gate  $R_{XYX}(-\pi/4)$  is appended at the right end.

$Z$ -rotation gates with arbitrary angles, without loss of generality.

### III. THEORY OF MULTI-PRODUCT COMMUTATION RELATION

In this section, we present the multi-product commutation relation (MCR), a nontrivial commutation rule that enables certain groups of non-commuting multi-Pauli rotation gates to be reordered. We also establish the necessary and sufficient conditions for MCR construction and show how MCR enables circuit simplification beyond the reach of local optimization rules.

#### A. Definition of MCR

We define each segment of sequential PBC, separated by dotted lines in Fig. 6, as a  $T$  layer [30].

**Definition 1** ( $T$  layer). *In sequential PBC, a segment is called a  $T$  layer if:*

- (i) *All multi-Pauli rotation gates within the layer mutually commute.*
- (ii) *For any multi-Pauli rotation gate  $P$  in the  $(i+1)$ th layer, there exists at least one gate  $Q$  in the  $i$ th layer that anticommutes with  $P$ .*

If the rotation axes of non-Clifford gates match exactly in succession, their rotation angles can be combined into a single gate, resulting in  $T$ -count reduction by two, i.e.,  $R_P(\pm\pi/4)R_P(\pm\pi/4) = R_P(k\pi/2) \in \mathcal{C}_n$ . Such merging

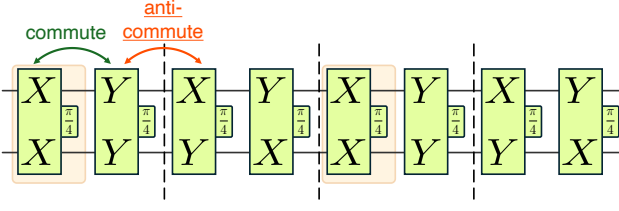


FIG. 6. A circuit containing adjacent Pauli rotation gates, some of which commute. However, due to intervening anti-commuting gates, no further gate merging for circuit optimization is possible.

optimization applies even to non-adjacent gates, provided they belong to the same  $T$  layer.  $T$ -count optimization compilers exploiting this gate synthesis rule in common  $T$  layers have been proposed [30, 32].

However, some circuits remain unsimplifiable under this approach. For example, the circuit in Fig. 6 contains four  $T$  layers. Within each layer, gates such as  $R_{XX}(\pi/4)$  and  $R_{YY}(\pi/4)$  or  $R_{XY}(\pi/4)$  and  $R_{YX}(\pi/4)$ , commute with each other. In contrast, gates across adjacent layers such as  $R_{YY}(\pi/4)$  and  $R_{XY}(\pi/4)$  anticommute, making them unswappable and preventing further optimization. Applying MCR overcomes this limitation, i.e., certain gates can be swapped as composite units while preserving the overall circuit functionality. In the remainder of this section, we formalize this commutation rule in terms of multi-Pauli rotation axes and demonstrate its use in enabling nontrivial gate reordering.

We define the *multi-product commutation relation* (MCR) as a specific combination of multi-Pauli rotation gates whose axes satisfy certain commutation and anti-commutation conditions.

**Definition 2** (Multi-product commutation relation). *Let  $A, B, C, D \in \mathcal{P}_n^*$  be mutually distinct (up to a sign  $\pm 1$ ) multi-Pauli axes corresponding to the rotation gates with an angle of  $\pi/4$ . We say that the pairs  $(R_A, R_B)$  and  $(R_C, R_D)$  satisfy the multi-product commutation relation (MCR) if the following three conditions hold:*

1.  $[A, B] = [C, D] = 0$ ,
2.  $\{A, C\} = \{A, D\} = \{B, C\} = \{B, D\} = 0$ ,
3.  $[A + B, C + D] = 0$ .

Here,  $[M_1, M_2] := M_1M_2 - M_2M_1$  denotes the commutator and  $\{M_1, M_2\} := M_1M_2 + M_2M_1$  denotes the anti-commutator.

**Theorem 1.** *Any sequential PBC whose axes satisfy the MCR can be entirely swapped. That is, for  $(R_A, R_B)$  and  $(R_C, R_D)$  satisfying Definition 2, Eq. (11) holds as shown in Fig. 7.*

$$\begin{aligned} R_D\left(\frac{\pi}{4}\right)R_C\left(\frac{\pi}{4}\right)R_B\left(\frac{\pi}{4}\right)R_A\left(\frac{\pi}{4}\right) \\ = R_B\left(\frac{\pi}{4}\right)R_A\left(\frac{\pi}{4}\right)R_D\left(\frac{\pi}{4}\right)R_C\left(\frac{\pi}{4}\right) \end{aligned} \quad (11)$$

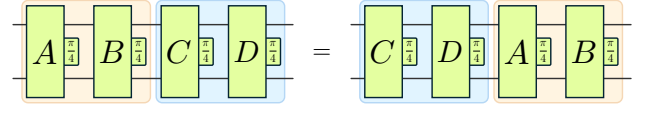


FIG. 7. Circuit diagram illustrating the gate sequence satisfying MCR.

*Proof.* From conditions 1 and 3 of Definition 2, we have

$$\begin{aligned} R_D\left(\frac{\pi}{4}\right)R_C\left(\frac{\pi}{4}\right)R_B\left(\frac{\pi}{4}\right)R_A\left(\frac{\pi}{4}\right) \\ = e^{-i\frac{\pi}{8}(D+C)}e^{-i\frac{\pi}{8}(B+A)} \\ = e^{-i\frac{\pi}{8}(B+A)}e^{-i\frac{\pi}{8}(D+C)} \\ = R_B\left(\frac{\pi}{4}\right)R_A\left(\frac{\pi}{4}\right)R_D\left(\frac{\pi}{4}\right)R_C\left(\frac{\pi}{4}\right). \end{aligned} \quad (12)$$

□

Note that condition 2 of Definition 2 is not explicitly used in the above derivation. Instead, it serves to exclude the trivial case where all pairs among  $R_A, R_B, R_C$ , and  $R_D$  commute. In this case, the gates can be freely reordered, and the commutation relation becomes obvious. Condition 2 ensures that the MCR captures only nontrivial gate reorderings that cannot be justified by pairwise commutation alone.

Consider the circuit shown in Fig. 8, where Theorem 1 enables a nontrivial gate reordering that leads to further optimization. The circuit remains equivalent even if the pairs  $(R_{XY}, R_{YX})$  and  $(R_{XX}, R_{YY})$  are swapped, since these four gates satisfy all conditions in Definition 2. After performing this swap, the sequence of rotation axes becomes  $XX, YY, XX, YY, XY, YX, XY, YX$ . Since  $[XX, YY] = 0$  and  $[XY, YX] = 0$ , the respective pairs are pairwise commutable. This observation allows each adjacent pair to be merged into a single Clifford gate, resulting in the simplified sequence:  $R_{XX}(\pi/2), R_{YY}(\pi/2), R_{XY}(\pi/2), R_{YX}(\pi/2)$ . This example illustrates how MCR enables circuit simplification beyond local rewrite rules by capturing a broader class of gate rearrangement of multi-Pauli rotations.

## B. Systematic design of sequential PBC satisfying MCR

We now explain a method that enables efficient construction of sequential PBC satisfying MCR. The following theorem provides the requirements under which four distinct rotation axes give rise to an MCR construction.

**Theorem 2** (Construction of rotation axes satisfying MCR). *Let  $A, B, C, D \in \mathcal{P}_n^*$ , and let all rotation angles be  $\pi/4$ . Here,  $A, B, C, D$  are assumed to have mutually distinct rotation axes, up to a sign  $\pm 1$ . Suppose  $A, B, C$  satisfy  $[A, B] = 0$  and  $\{A, C\} = \{B, C\} = 0$ . Then, the following (I) and (II) are equivalent.*

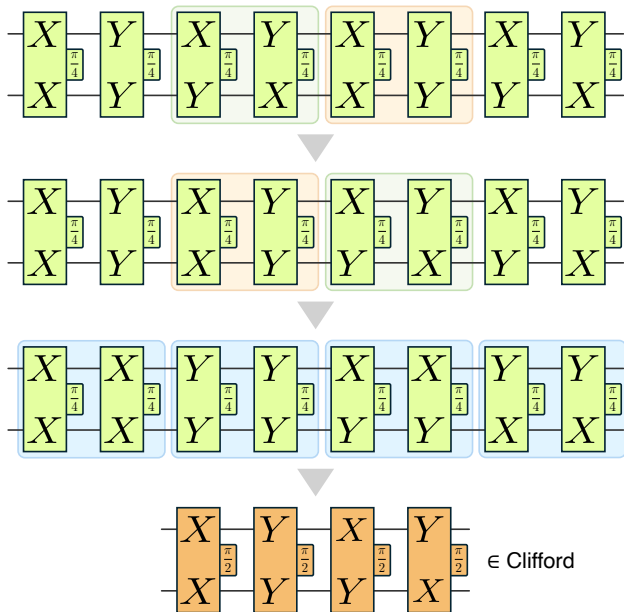


FIG. 8. Optimization of the circuit shown in Fig. 6 using MCR condition. The circuit remains equivalent under the swap of commuting pairs,  $(R_{XX}(\pi/4), R_{YY}(\pi/4))$  and  $(R_{XY}(\pi/4), R_{YX}(\pi/4))$ . After rearrangement, the circuit is partitioned into two  $T$  layers consisting of four gates each. Within each  $T$  layer, gates with shared rotation axes can be merged into Clifford gates. As a result, the entire circuit is reduced to a form that can be expressed using only Clifford operations.

(I)  $A, B, C$ , and  $D$  satisfy all of the following (i)–(iii).

(i)  $[C, D] = 0$ ,

(ii)  $\{A, D\} = \{B, D\} = 0$ ,

(iii)  $[A + B, C + D] = 0$ .

(II)  $D = -ABC$ .

*Proof.* See Appendix A.  $\square$

Theorem 2 provides a constructive method for generating rotation axes that satisfy MCR. For instance, in the circuit from Fig. 6, we can set  $A = XY$ ,  $B = YX$ , and  $C = XX$ . Then,  $-ABC = YY$ , confirming that the rotation axis of the fourth gate satisfies  $D = -ABC$ . While this example involves two-qubit multi-Pauli rotation gates, we can apply MCR to  $n$ -qubit multi-Pauli rotation gates as well. In this case, the total number of combinations of rotation axes that satisfy MCR grows exponentially with  $n$ . For details, see Appendix B.

#### IV. COMPILER BENCHMARK USING MCR

In this section, we introduce the concept of quantum circuit unoptimization, an operation that transforms a

circuit into a more complex one while preserving its overall functionality. Subsequently, we present a method for generating benchmark datasets to verify whether MCR described in Sec. III constitutes a nontrivial equivalent transformation not included in existing  $T$  gate optimization compilers. We also describe a quantitative evaluation method for compiler performance using the  $T$ -count as a metric.

##### A. Quantum circuit unoptimization

We use the term *quantum circuit unoptimization* to describe the process of deliberately introducing gate redundancies while keeping the circuit equivalent. The following definition formalizes this concept.

**Definition 3** (Quantum circuit unoptimization [34]). *Quantum circuit unoptimization is the process of generating a redundant  $n$ -qubit circuit  $V$  from an  $n$ -qubit circuit  $U$ , as expressed by:*

$$V = \mathcal{O}(U, C). \quad (13)$$

$C$  is a recipe constructed from elements of the set of basic unoptimization operations  $\mathcal{S}$ .  $\mathcal{O}$  is a function (Unoptimizer) that transforms  $U$  into  $V$  based on the information in  $C$ . We assume that both  $U$  and  $V$  are poly( $n$ ) gates, and the operation generating  $V$  from  $U$  can be efficiently executed on a classical computer. If the conditions for unoptimization are satisfied,  $V$  is equivalent to  $U$  up to a global phase  $\phi$ , i.e.,

$$V^\dagger U = e^{i\phi} I \quad (14)$$

where  $I$  represents the  $n$ -qubit identity operator.

Figure 9 illustrates a diagram of quantum circuit unoptimization. Given an input quantum circuit  $U$ , a more complex quantum circuit  $V$  is generated by applying a recipe that describes how to introduce redundancy. To define such a recipe, it is necessary to determine the set of allowed basic unoptimization operations  $\mathcal{S}$ . Note that only circuit operations that preserve the equivalence of the quantum circuit before and after the operation can be included in  $\mathcal{S}$ . The complexity of the unoptimized circuit depends critically on the choice of  $\mathcal{S}$ . For example, if we take  $\mathcal{S} = \{\text{Insert two } X \text{ gates at random positions in the circuit}\}$ , this satisfies the condition that the unoptimization operations preserve circuit equivalence. However, such redundancy is trivial: any compiler that recognizes  $X^2 = I$  will immediately remove the inserted gates. To generate more meaningful redundancy, we set  $\mathcal{S} = \{\text{Gate insertion, Gate swapping}\}$ . By appropriately composing these operations, we create a recipe to construct circuits that are challenging for compilers to optimize.

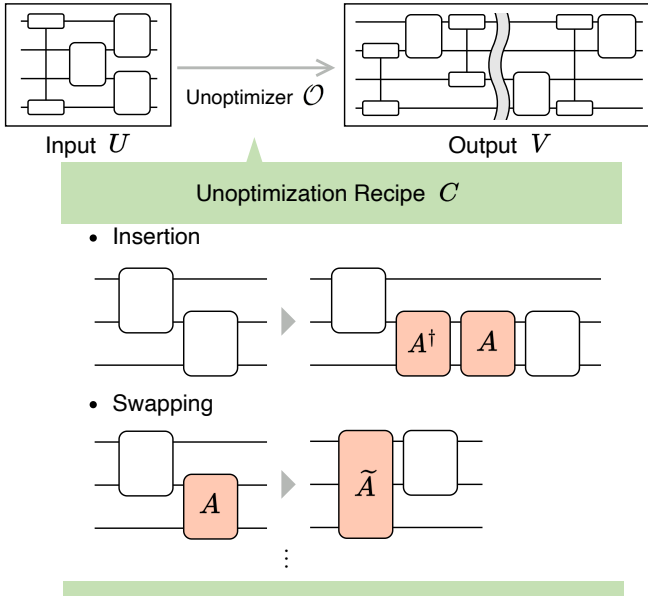


FIG. 9. Schematic illustration of quantum circuit unoptimization. The basic operations consist of gate insertion and gate swapping, which are used to construct an unoptimization recipe. Applying this recipe to an input circuit  $U$  produces a redundant circuit  $V$  that is equivalent to  $U$  up to a global phase.

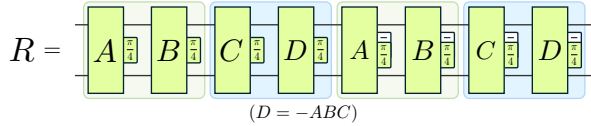


FIG. 10. Construction of a quantum circuit that implements the identity operator by leveraging the MCR property. Each alphabet represents a rotation axis of a multi-Pauli rotation.

## B. MCR-based recipes for unoptimization

First, we explain *gate insertion*, which refers to the operation of inserting a gate  $A$  together with its inverse  $A^\dagger$  placed adjacently in the circuit, yielding the identity operator. A typical example is the insertion of  $R_P(\theta)$  followed by  $R_P(-\theta)$ . In this paper, we generalize this concept by employing MCR to construct more complex identity sequences, denoted  $R$ , as depicted in Fig. 10. Such sequences are systematically generated by selecting rotation axes satisfying the MCR conditions and arranging their gates and inverses, as formalized in Theorem 2. An example is shown in Fig. 11, and the generation procedure is given in Algorithm 1.

Next, we explain the operation of *gate swapping*, which refers to exchanging the positions of two adjacent gate blocks in a circuit. Here, we combine the gate swapping with an additional gate insertion that induces commutativity through MCR. This procedure is illustrated in Fig. 12. Consider the swap of the rightmost two gates

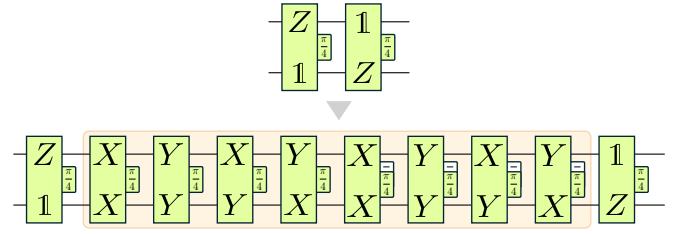


FIG. 11. A gate insertion example based on Fig 10. Although the inserted circuit is equivalent to the identity, it cannot be simplified by considering only pairwise commutativity of adjacent gates.

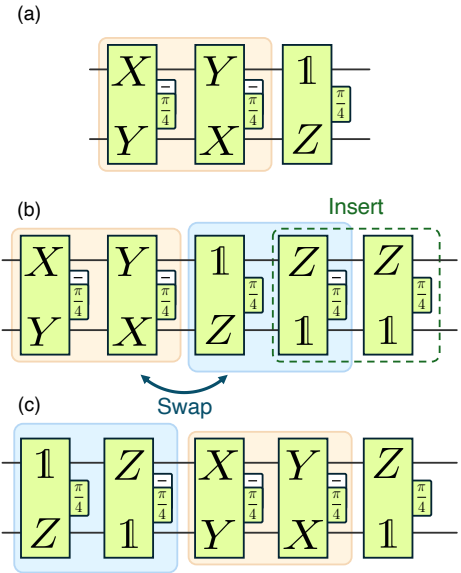


FIG. 12. Gate swapping unoptimization based on MCR. (a) The circuit segment after the gate insertion. (b) Additional gate insertion of identity gates (green dashed box) to satisfy MCR. (c) The resulting circuit after swapping the commuting blocks.

in the 8-gate identity sequence constructed via MCR (as shown in Fig. 11) with the gate immediately to their right. Since MCR can only be applied to pairs of gates, it is necessary to add one more gate to complete the MCR condition. This supplementary gate can be computed using Theorem 2; in this case,  $-ABC = -ZI$ . Therefore, by adding  $R_{ZI}(-\pi/4)$ , a gate sequence satisfying MCR can be constructed. Thus, as shown in Fig. 12(b), if we insert  $R_{ZI}(-\pi/4)$  and  $R_{ZI}(\pi/4)$  to the right of  $R_{YX}(-\pi/4)$ , we can swap the two pairs of gates ( $R_{XY}(-\pi/4), R_{YX}(-\pi/4)$ ) and ( $R_{IZ}(\pi/4), R_{ZI}(-\pi/4)$ ) since they satisfy MCR. The resulting reordered sequence is shown in Fig. 12(c).

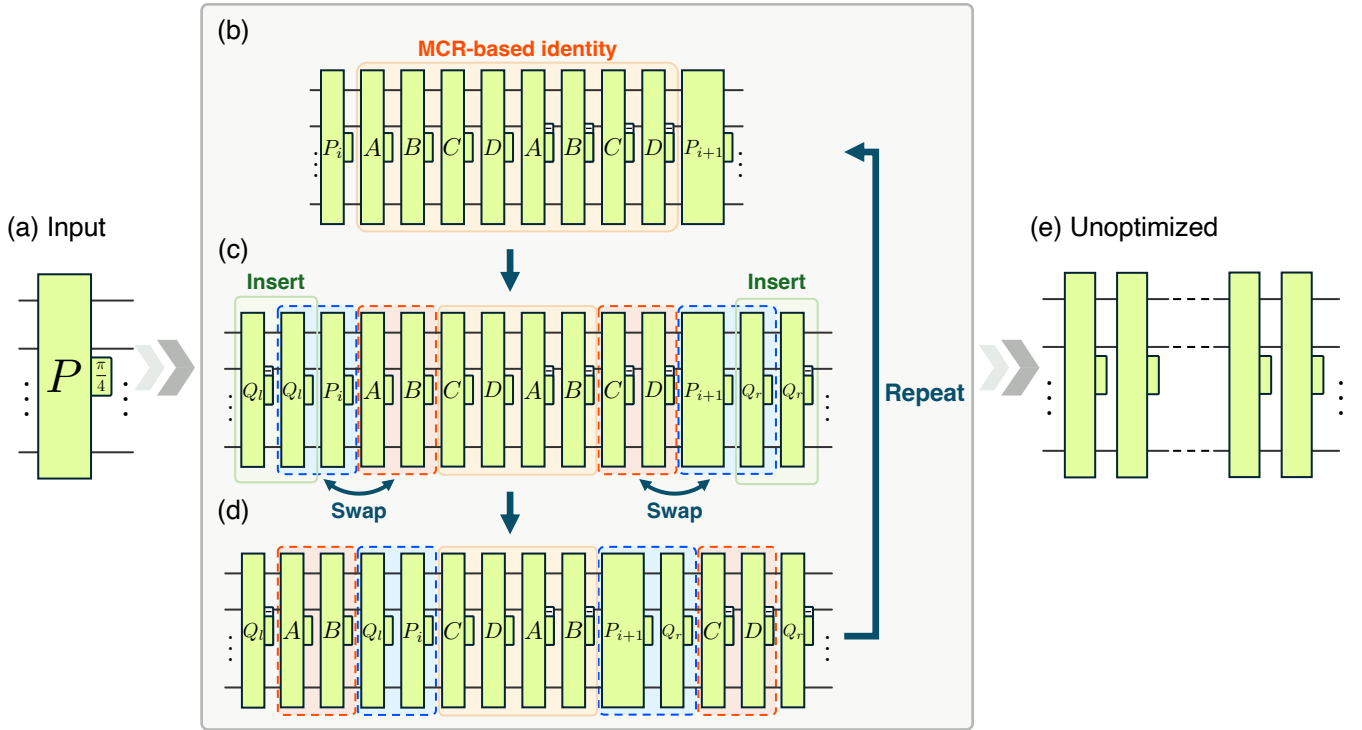


FIG. 13. Overview of MCR-based quantum circuit unoptimization. (a) The input circuit, consisting of a single multi-Pauli rotation gate. (b) Insertion of an MCR-based identity sequence (as constructed in Fig. 10). (c) Insertion of additional gates  $R_{Q_i}^\dagger$  and  $R_{Q_i}$  at both ends, corresponding to the procedure described in Fig. 12(b). (d) The circuit after swapping the outermost gates, thereby completing the procedure in Fig. 12. (e) The unoptimized circuit obtained by repeating steps (b) – (d)  $n^2$  times.

---

**Algorithm 1** MCR-based quantum circuit unoptimization

---

- 1: **Generation of identity operator using MCR**
  - 2: Select  $A \in \mathcal{P}_n^*$
  - 3: Choose  $B \in \mathcal{P}_n^*$  such that  $[A, B] = 0$
  - 4: Choose  $C \in \mathcal{P}_n^*$  such that  $\{A, C\} = 0$  and  $\{B, C\} = 0$
  - 5: Compute  $D \leftarrow -ABC$
  - 6: Construct gate sequence:
 
$$R \leftarrow R_{-D}(\pi/4)R_{-C}(\pi/4)R_{-B}(\pi/4)R_{-A}(\pi/4) \\ R_D(\pi/4)R_C(\pi/4)R_B(\pi/4)R_A(\pi/4)$$
  - 7: **Output:** Gate sequence  $R$  such that  $R = I$
  - 8:
  - 9: **Generation of unoptimized circuit**
  - 10: **for**  $i \leftarrow 0$  to  $n^2 - 1$  **do**
  - 11:    $C[i] \leftarrow R$ , Gate Swapping
  - 12: **end for**
  - 13:  $V \leftarrow \mathcal{O}(U, C)$
- 

**C. Procedure for benchmark circuit construction**

We explain the unoptimization algorithm that combines the gate insertion and gate swapping techniques described above, along with the compiler benchmarking methodology. The overall workflow is illustrated in Fig. 13. We begin with an  $n$ -qubit circuit  $U$  consisting of

---

**Algorithm 2** Compiler benchmark

---

- 1: **Input:**  $n$ -qubit circuit  $U$
  - 2: Obtain an unoptimized circuit  $V$  using **Algorithm 1**
  - 3: Decompose  $U$  into a Clifford+ $T$  gate set
  - 4: Obtain  $T$ -count:  $t_{\text{original}}$
  - 5: Decompose  $V$  into a Clifford+ $T$  gate set
  - 6: Obtain  $T$ -count:  $t_{\text{unopt}}$
  - 7: Apply  $T$  gate optimization compiler to  $V$
  - 8: Obtain optimized  $T$ -count:  $t_{\text{opt}}$
  - 9: Compute gate reduction rate:  $p$
  - 10:  $p \leftarrow (t_{\text{unopt}} - t_{\text{opt}})/(t_{\text{unopt}} - t_{\text{original}})$
  - 11: **Output:**  $t_{\text{unopt}}, t_{\text{opt}}, p$
- 

a single multi-Pauli rotation gate  $R_P(\pi/4)$ , which guarantees an optimal  $T$ -count of 1 and thus cannot be further reduced. Then, from the circuit, we randomly select one multi-Pauli rotation gate  $P_i$  and insert an identity operator based on Algorithm 1 immediately to its right. We make the identity sequence such that the following conditions are satisfied:

$$\{P_i, A\} = \{P_i, B\} = \{C, P_{i+1}\} = \{D, P_{i+1}\} = 0. \quad (15)$$

Next, we perform gate swapping on the two gates at both ends of the inserted gate sequence. Here, we first explain the operation of the gates in the left half. In

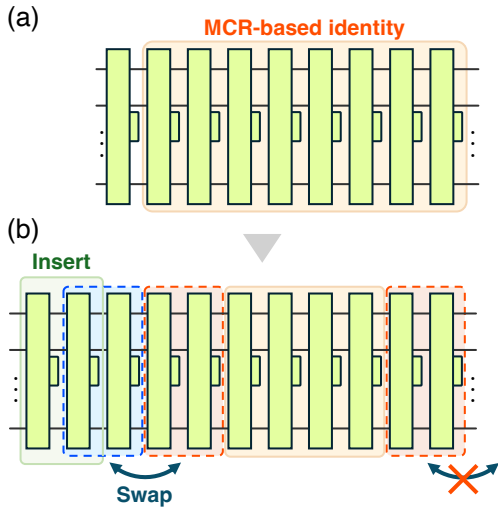


FIG. 14. Special case of gate swapping in MCR-based unoptimization when the target gate is located at the rightmost end of the circuit. (a) Circuit after inserting an MCR-based identity operator. (b) Swap operation applied only to the left end, as the right end cannot be operated in this configuration.

Fig. 13(c), we insert an additional gates  $R_{Q_i}(-\pi/4)$  and  $R_{Q_i}(\pi/4)$  (highlighted in green), where  $Q_i = -P_iAB$ . Since the gate pairs  $(R_{Q_i}, R_{P_i})$  (highlighted in blue) and  $(R_A, R_B)$  (highlighted in red) satisfy MCR, we can swap these pairs. This operation results in the updated gate sequence depicted in Fig. 13(d). We perform a similar operation on the gate sequence in the right half. In this case,  $Q_r = -CDP_{i+1}$ , which also satisfies MCR with the adjacent pairs  $(R_{-C}, R_{-D})$  and  $(R_{P_{i+1}}, R_{Q_r})$ . Note that when we select the gate  $P_i$  as the right edge of the circuit, we swap the gates on only the left side as shown in Fig. 14. In this case, we do not add the additional gates  $R_{Q_r}(\pi/4), R_{Q_r}(-\pi/4)$ , and only the left-side gates are swapped with the inserted gate sequence.

We repeat these procedures  $n^2$  times, where  $n$  is the number of qubits in the circuit. The final circuit obtained is the unoptimized circuit  $V$ , as shown in Fig. 13(e). The gate insertion and swapping methods enable the systematic transformation of a simple input circuit into a structurally distinct one by changing the type, position, and order of the inserted gates. In our implementation, identity sequences are randomly generated using Algorithm 1. If the resulting sequence does not satisfy the anticommution conditions required for MCR-based gate swapping (Eq. (15)), the generation step is repeated until a valid candidate is found.

#### D. Numerical experiments

We present numerical experiments evaluating how well existing compilers can optimize circuits containing MCR-based gate structures. We focus on four  $T$  gate optimiza-

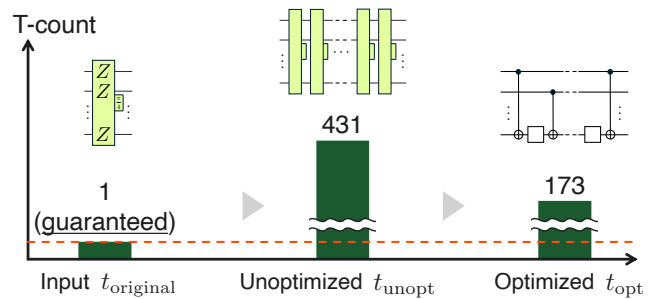


FIG. 15. An example workflow for assessing quantum compiler performance using an unoptimized benchmark circuit. The input circuit is the rotation  $R_{ZZ\dots Z}(\pi/4)$ , whose theoretical  $T$ -count is 1 (indicated by the red dashed line). In this illustrative case, applying Algorithm 2 produces an unoptimized Clifford+ $T$  circuit  $V$  with  $t_{\text{unopt}} = 431$ . We then decompose  $V$  into a Clifford+ $T$  gate set and pass the resulting circuit to a compiler. This yields an optimized circuit with  $t_{\text{opt}} = 173$ , corresponding to a 60%  $T$ -count reduction as defined in Eq. (16).

tion compilers: Pytket, PyZX, TMerge, and FastTODD. To assess compiler performance, we use the unoptimized circuit  $V$  generated by Algorithm 1 as input. We explain how to evaluate compiler performance using the unoptimized circuit  $V$  generated by Algorithm 2. A workflow of this benchmark task is illustrated in Fig. 15. Each unoptimized circuit has a  $T$ -count denoted as  $t_{\text{unopt}}$  and is passed to a compiler for optimization, resulting in a circuit with  $T$ -count  $t_{\text{opt}}$ . We quantify the optimization performance using the  $T$ -count reduction rate  $p$  defined as

$$p = \frac{t_{\text{unopt}} - t_{\text{opt}}}{t_{\text{unopt}} - t_{\text{original}}}. \quad (16)$$

Here,  $t_{\text{original}}$  is the  $T$ -count of the input circuit before unoptimization. In this paper, we use the single multi-Pauli rotation gate  $R_{ZZ\dots Z}(\pi/4)$  as the input circuit, which has a theoretical  $T$ -count of 1, i.e.,  $t_{\text{original}} = 1$ . A larger value of  $t_{\text{unopt}}$  indicates a higher degree of unoptimization. The greater the difference between  $t_{\text{unopt}}$  and  $t_{\text{opt}}$ , the better the performance of the compiler, which corresponds to a higher value of  $p$ . Since  $p$  is normalized by the maximum possible reduction in  $T$ -count, it always falls within the range of 0 to 1. In particular,  $p = 1$  indicates perfect optimization, where the compiler completely restores the original circuit.

We use the following four state-of-the-art  $T$ -gate optimization compilers in our experiments:

1. Pytket [18]

Developed by Quantinuum, Pytket is a general-purpose compiler that supports optimization for NISQ devices. Although its primary focus is on circuit depth reduction, it also includes a  $T$ -count optimization pass. In our experiments, we use `RemoveRedundancies` to eliminate unnecessary  $T$  gates.

## 2. PyZX [35]

PyZX applies optimization techniques based on ZX-calculus, which represents a quantum circuit as a graphical diagram. It includes graph-theoretic optimization techniques such as local complementation and pivoting [21, 22] using  $X$ -Spiders and  $Z$ -Spiders. We use `full_reduce` function for maximum simplification in the ZX-diagram, and then convert it back to a quantum circuit.

## 3. TMerge [32]

TMerge reduces the  $T$ -count by exploiting the commutativity of Pauli rotation axes. As described in Sec. II B, it first separates the input Clifford+ $T$  circuit into a Clifford gate sequence and a sequential PBC. This compiler can reorder them within each  $T$  layer and merge rotation gates that have the same axis.

## 4. FastTODD [27]

FastTODD uses phase-polynomial as an IR and optimizes the  $T$ -count by solving the symmetric tensor rank decomposition problem [36]. It removes all internal Hadamard gates by introducing ancilla qubits and applies a fast version of the Third Order Duplicate and Destroy (TODD) algorithm [26] to minimize the  $T$ -count.

We create the benchmark circuits via quantum circuit unoptimization using the quantum circuit simulator Stim [37]. We can entirely characterize the type of a multi-Pauli rotation gate by a Pauli string specifying the rotation axis and a sign indicating whether the rotation angle is  $\pi/4$  or  $-\pi/4$ . Stim is well-suited for dealing with such circuits, as it allows efficient updates of Pauli strings under Clifford conjugation while preserving small representations. Since the unoptimized circuit consists solely of multi-Pauli rotation gates with angles of  $\pm\pi/4$ , they can be exactly decomposed into Clifford+ $T$  gates. To save benchmark circuit data, we use the Qasm [38] and qc file formats [39]. To ensure that the unoptimization process preserves circuit equivalence as defined in Eq. (14), we verify correctness using the MQT-qcec tool provided by The Munich Quantum Toolkit [40]. All source code used in this work is available on GitHub [41].

Table I summarizes the averaged results. The table includes the  $T$ -count before optimization, followed by the output from each compiler: the reduced  $T$ -count and the corresponding reduction percentage. For FastTODD, an additional column shows the number of ancilla qubits  $n_h$  introduced via Hadamard gadgetization. As expected, we verify that the  $T$ -counts  $t_{\text{unopt}}$  and  $t_{\text{opt}}$  increase as the number of qubits  $n$  increases. Among the compilers, FastTODD consistently achieves the most substantial reductions. For instance, at  $n = 2$ , it reduces the  $T$ -count by over 33%. However, its effectiveness drops as  $n$  increases, reaching 0% at  $n = 9$ . Moreover, FastTODD introduces a large number of ancilla qubits  $n_h$  during Hadamard gadgetization. For example, at  $n = 9$ ,

it requires over 630 ancilla qubits, increasing the total number of qubits by more than 70 times. Compilation becomes computationally expensive at this scale, with runtimes exceeding 21 hours per circuit, despite yielding no improvement in  $T$ -count. In comparison, PyZX and TMerge provide modest reductions for small circuits, but their performance similarly degrades as  $n$  grows, with both reaching 0% reduction at  $n = 9$ . Pytket, on the other hand, consistently shows a relatively lower reduction rate compared to other compilers.

To explore why optimization partially works for small circuits but not for larger ones, we conduct an additional numerical experiment using a benchmark dataset generated by skipping step (c) in Fig. 13, i.e., omitting gate swapping based on MCR. We report the results in Table II, revealing a complete absence of  $T$ -count reduction across compilers and circuit sizes. Even FastTODD, despite the introduction of ancilla qubits, fails to achieve any improvement under this condition. This result suggests that for circuits with a small number of qubits, MCR-based gate swapping accidentally matches the rotation axes of neighboring gates, making optimization easier. Since the total number of gate sequences satisfying MCR increases exponentially with the number of qubits  $n$  (see Appendix B for details), cases where the rotation axes coincide after swapping become less likely as  $n$  increases.

From the above results, we demonstrate that by performing unoptimization based on MCR, it is possible to generate quantum circuits that existing compilers cannot efficiently optimize. In other words, MCR constitutes an equivalent transformation rule that is not incorporated into current compilers.

## V. CONCLUSION AND OUTLOOK

In this paper, we propose and formalize the multi-product commutation relation (MCR) as a nonlocal and ancilla-free circuit transformation rule for Clifford+ $T$  circuits. MCR enables equivalent rewrites involving multiple non-adjacent multi-Pauli rotation gates, capturing nontrivial commutativity that pairwise commutation rules cannot reach. Given the rotation axes of three multi-Pauli rotation gates, Theorem 2 provides a concrete condition to determine the fourth gate that satisfies MCR. We leverage this property to a procedure called quantum circuit unoptimization, which introduces redundancy into Clifford+ $T$  circuits by inserting and swapping quantum gates while preserving circuit equivalence. This approach systematically generates complex circuits from simple ones with a guaranteed optimal  $T$ -count, offering a quantitative framework for evaluating how well a compiler eliminates redundant  $T$  gates.

Through numerical experiments, we demonstrate that circuits transformed using MCR-based unoptimization are challenging for existing  $T$ -count optimization compilers to optimize, suggesting that MCR offers circuit

TABLE I. Comparison of  $T$  gate optimization results across four compilers.  $T$ -counts before ( $t_{\text{unopt}}$ ) and after ( $t_{\text{opt}}$ ) optimization are shown for quantum circuits with  $n$  qubits. The percentage reduction in  $T$ -count is denoted as Red. (%). For FastTODD,  $n_h$  indicates the number of ancilla qubits introduced during Hadamard gadgetization. We report the optimization results averaged over 100 samples.

$n$	$t_{\text{unopt}}$	Pytket		PyZX		TMerge		FastTODD		
		$t_{\text{opt}}$	Red. (%)	$t_{\text{opt}}$	Red. (%)	$t_{\text{opt}}$	Red. (%)	$t_{\text{opt}}$	$n_h$	Red. (%)
2	46.68	42.96	8.14	31.80	32.53	31.80	32.53	31.54	18.23	<b>33.10</b>
3	106.38	104.22	2.05	95.68	10.15	95.68	10.15	94.90	58.64	<b>10.89</b>
4	190.42	189.24	0.62	185.06	2.83	185.06	2.83	184.36	116.21	<b>3.20</b>
5	298.34	297.94	0.14	296.22	0.71	296.22	0.71	295.82	188.82	<b>0.85</b>
6	430.34	430.30	0.0093	429.72	0.14	429.72	0.14	429.68	278.55	<b>0.15</b>
7	586.38	586.36	0.0034	586.20	0.031	586.20	0.031	586.16	382.82	<b>0.038</b>
8	766.26	766.26	0.00	766.24	0.0026	766.24	0.0026	766.16	502.94	<b>0.013</b>
9	970.10	970.10	0.00	970.10	0.00	970.10	0.00	970.10	637.52	0.00

TABLE II. Comparison of  $T$  gate optimization results across four compilers without MCR-swap. The same definitions for  $t_{\text{unopt}}$ ,  $t_{\text{opt}}$ , and  $n_h$  apply as in Table I.

$n$	$t_{\text{unopt}}$	Pytket		PyZX		TMerge		FastTODD		
		$t_{\text{opt}}$	Red. (%)	$t_{\text{opt}}$	Red. (%)	$t_{\text{opt}}$	Red. (%)	$t_{\text{opt}}$	$n_h$	Red. (%)
2	33.00	33.00	0.00	33.00	0.00	33.00	0.00	33.00	18.95	0.00
3	73.00	73.00	0.00	73.00	0.00	73.00	0.00	73.00	47.40	0.00
4	129.00	129.00	0.00	129.00	0.00	129.00	0.00	129.00	87.07	0.00
5	201.00	201.00	0.00	201.00	0.00	201.00	0.00	201.00	138.80	0.00
6	289.00	289.00	0.00	289.00	0.00	289.00	0.00	289.00	202.45	0.00
7	393.00	393.00	0.00	393.00	0.00	393.00	0.00	393.00	277.03	0.00
8	513.00	513.00	0.00	513.00	0.00	513.00	0.00	513.00	364.01	0.00
9	649.00	649.00	0.00	649.00	0.00	649.00	0.00	649.00	461.18	0.00

rewrites that remain unexplored by existing compilation strategies. We also compare the optimization performance results with and without MCR-based gate swapping. The comparison shows that while MCR-based gate swapping introduces additional circuit redundancy, it can occasionally trigger effective local optimization in small regions of the circuit. However, such cases become infrequent as the number of qubits grows, due to the exponential increase in the number of valid MCR candidates.

MCR involves circuit transformations that can increase or decrease the number of  $T$  layers, thereby suggesting a broader class of rewrite rules beyond the reach of existing compiler strategies. This insight opens opportunities for compiler design, circuit synthesis, and algorithm-based optimization. A key direction for future work is to design a compiler that incorporates an MCR-based gate swapping technique toward further  $T$ -count reduction. However, simply adding such a rule to existing optimization passes is not sufficient, since the number of possible MCR candidates grows exponentially with the system size, making brute-force exploration computationally infeasible. Addressing this challenge requires developing a search strategy that partitions the circuit into manageable subcircuits and selectively explores promising regions. Once developed, the performance of such a compiler can be evaluated on representative datasets, such as the *Reversible Benchmarks* [39].

Another promising direction involves generalizing MCR to Clifford+ $R_Z$  circuits with continuous rotation angles. This circuit class is widely used in quantum algorithms, including variational quantum algorithms [42, 43] and Trotterized quantum simulation tasks [44]. In architectures that support transversal Clifford gates and implement  $Z$ -rotations using repeat-until-success protocols, minimizing the number of such gates can significantly improve execution efficiency [45, 46]. Consequently, many quantum algorithms can benefit from an MCR-based optimization tool designed to reduce them. The authors in Ref. [47] propose a method to optimize the number of parameters in non-repeated parameterized quantum circuits. However, this excludes circuits where parameters exhibit algebraic relationships, such as the simultaneous appearance of  $\alpha_1$  and  $-\alpha_1 + \pi/4$ . In contrast, MCR admits simplifications even in these correlated cases, offering opportunities to optimize beyond the reach of current techniques. This property may provide value in structured algorithms, such as QAOA-MC [48], where repeated parameters are present.

For circuits using discrete angles, also known as Clifford+ $R_Z(\pi/2^k)$  circuits, which relate closely to the Clifford hierarchy [49, 50], MCR could offer similar benefits. Prior works [25, 27] explore optimization in this setting using Reed-Muller code techniques and prove that this problem can be reduced to the higher-order symmet-

ric tensor rank decomposition problem. The complexity of the symmetric tensor rank decomposition problem remains unknown. However, the related problem of determining the tensor rank of a third-order tensor, without the symmetry constraint, is NP-complete [51]. We expect MCR-based strategies to improve the compilation performance even in such a circuit structure. A practical application in this circuit setting is time evolution by probabilistic angle interpolation (TE-PAI) [52], which simulates quantum dynamics using ensembles of random circuits composed only of multi-Pauli rotations with angles  $\pm\Delta$  or  $\pm\pi$ . Since these circuits belong to the Clifford+ $R_Z$  (discrete angle) class, a compiler that reduces redundant rotations could help efficiently implement TE-PAI on a real quantum device.

### ACKNOWLEDGEMENT

This work is supported by the MEXT Quantum Leap Flagship Program (MEXT Q-LEAP) Grant No. JPMXS0120319794, JST COI-NEXT Grant No. JPMJPF2014, JST Moonshot R&D Grant No. JPMJMS2061, and JSPS KAKENHI Grant No. JP25KJ1712 and JP24K16979.

### Appendix A: Proof of Theorem 2

We prove Theorem 2 as described in Sec. III B.

( $\Leftarrow$ ) This can be demonstrated by substituting  $D = -ABC$  into (i)–(iii) of (I) in order.

( $\Rightarrow$ ): Combining (ii) and (iii) of (I) and the given assumptions, we obtain

$$\begin{aligned} [A + B, C + D] &= 0 & (\text{A1}) \\ \Rightarrow AC + AD + BC + BD &= 0 & (\text{A2}) \end{aligned}$$

Since  $A, B, C$ , and  $D$  are mutually distinct Pauli operators, each term in Eq. (A2) is a non-identity Pauli product. Because the set of  $n$ -qubit Pauli operators forms an orthogonal basis under the Hilbert–Schmidt inner product, their sum can be zero only if terms cancel in pairs.

Case 1  $AC + BC = 0$   
Eq. (A2) becomes

$$\begin{aligned} AD + BD &= 0 & (\text{A3}) \\ \Rightarrow A &= -B, \end{aligned}$$

which implies that  $A$  and  $B$  have the same rotation axis but opposite rotation angles, contradicting the assumption that they have distinct axes.

Case 2  $AC + BC \neq 0$

We must partition the sum  $-(AC + BC)$  into two Pauli operators  $AD$  and  $BD$  such that their sum equals this value. Because a sum of two distinct Pauli operators cannot be another single Pauli operator, the only possibility is that  $(AD, BD) = (-AC, -BC)$  or  $(AD, BD) = (-BC, -AC)$ . We analyze these two cases separately.

- If  $(AD, BD) = (-AC, -BC)$ , then  $D = -C$ , implying that  $D$  and  $C$  share the same rotation axis, which again contradicts the assumption.
- If  $(AD, BD) = (-BC, -AC)$ , then  $D = -ABC (= -BAC)$ , which has a rotation axis distinct from all of  $A, B$ , and  $C$ , and hence satisfies the assumption.

Therefore, the only valid solution is  $D = -ABC$ .

### Appendix B: Analysis of the number of possible MCR pairs

Here, we explain the total number of combinations of gate rotation axes that satisfy MCR. MCR is a commutation rule applied to four sequential gates: two on the left and two on the right. Let the set of rotation axes be  $\mathcal{P}_n^* := \{\pm 1\} \times \{I, X, Y, Z\}^{\otimes n} \setminus \{\pm I^{\otimes n}\}$  (Eq. (8)), and let the rotation axes of the gates from the left be  $A, B, C, D \in \mathcal{P}_n^*$ , where each gate has a different rotation axis except for the sign  $\pm 1$ . According to Algorithm 1 in Sec. IV B, the method for choosing rotation axes that satisfy MCR is as follows.

1. Select one element from  $\mathcal{P}_n^*$  and set it as  $A$ .
2. Choose  $B \in \mathcal{P}_n^*$  such that  $B$  commutes with  $A$ .
3. Choose  $C \in \mathcal{P}_n^*$  such that  $\{A, C\} = \{B, C\} = 0$ .
4. Obtain  $D$  by setting  $D = -ABC$ .

Let us determine the number of ways to select the rotation axes according to this procedure. First, the axis  $A$  can be chosen from any non-identity Pauli operator, giving  $4^n - 1$  possible choices. The second axis  $B$  must commute with  $A$  and must not be equal to  $A$  or the identity. In general, for any given Pauli operator, half of the other operators commute with it. Therefore, the number of valid choices for  $B$  is  $4^n/2 - 2$ , where the subtraction accounts for excluding the identity operator and the previously chosen  $A$ . Next,  $C$  must anticommute with both  $A$  and  $B$ . Since one-fourth of all Pauli operators anticommute with both, the number of valid choices for  $C$  is  $4^{n-1}$ .  $D$  is determined uniquely as  $D = -ABC$  to satisfy MCR once  $A, B$ , and  $C$  are fixed as described in Theorem 2. Additionally, since the signs of  $A, B$ , and  $C$  can be chosen independently, we multiply by 8 to account for the possible sign combinations. However, to avoid overcounting due to permutation of the pairs  $(A, B)$  and  $(C, D)$ , and the exchange between these two pairs, we divide the total count by  $(2!)^3 = 8$ . Putting everything together, the total number of such combinations is

$$\frac{1}{8} \cdot 4^n (4^n - 1) (4^n - 4), \quad (\text{B1})$$

which shows that the number of possible axis configurations satisfying MCR scales exponentially with  $n$ .

- [1] P. W. Shor, Algorithms for quantum computation: discrete logarithms and factoring, in *Proceedings 35th Annual Symposium on Foundations of Computer Science* (1994) pp. 124–134.
- [2] L. K. Grover, A fast quantum mechanical algorithm for database search, in *Proceedings of the twenty-eighth annual ACM symposium on Theory of computing* (1996) pp. 212–219.
- [3] S. Lloyd, Universal quantum simulators, *Science* **273**, 1073 (1996).
- [4] I. M. Georgescu, S. Ashhab, and F. Nori, Quantum simulation, *Rev. Mod. Phys.* **86**, 153 (2014).
- [5] P. W. Shor, Fault-tolerant quantum computation, in *Proceedings of 37th Conference on Foundations of Computer Science* (IEEE, 1996) pp. 56–65.
- [6] Google Quantum AI and Collaborators, Quantum error correction below the surface code threshold, *Nature* **638**, 920 (2025).
- [7] M. A. Nielsen and I. L. Chuang, *Quantum Computation and Quantum Information: 10th Anniversary Edition* (Cambridge University Press, 2010).
- [8] S. Bravyi and A. Kitaev, Universal quantum computation with ideal Clifford gates and noisy ancillas, *Phys. Rev. A* **71**, 022316 (2005).
- [9] K. Svore, A. Aho, A. Cross, I. Chuang, and I. Markov, A layered software architecture for quantum computing design tools, *Computer* **39**, 74 (2006).
- [10] T. Häner, D. S. Steiger, K. Svore, and M. Troyer, A software methodology for compiling quantum programs, *Quantum Science and Technology* **3**, 020501 (2018).
- [11] F. T. Chong, D. Franklin, and M. Martonosi, Programming languages and compiler design for realistic quantum hardware, *Nature* **549**, 180 (2017).
- [12] V. A. Alfred, S. L. Monica, and D. U. Jeffrey, *Compilers principles, techniques & tools* (pearson Education, 2007).
- [13] V. Shende, S. Bullock, and I. Markov, Synthesis of quantum-logic circuits, *IEEE Transactions on Computer-Aided Design of Integrated Circuits and Systems* **25**, 1000 (2006).
- [14] C. M. Dawson and M. A. Nielsen, The solovay-kitaev algorithm, arXiv preprint quant-ph/0505030 (2005).
- [15] N. J. Ross and P. Selinger, Optimal ancilla-free Clifford+ $T$  approximation of  $z$ -rotations, arXiv preprint arXiv:1403.2975 (2014).
- [16] A. Cowtan, S. Dilkes, R. Duncan, A. Krajenbrink, W. Simmons, and S. Sivarajah, On the Qubit Routing Problem, in *14th Conference on the Theory of Quantum Computation, Communication and Cryptography (TQC 2019)*, Leibniz International Proceedings in Informatics (LIPIcs), Vol. 135, edited by W. van Dam and L. Mančinska (Schloss Dagstuhl – Leibniz-Zentrum für Informatik, Dagstuhl, Germany, 2019) pp. 5:1–5:32.
- [17] M. Treinish, J. Gambetta, D. M. Rodríguez, L. Bello, M. Marques, C. J. Wood, J. Gacon, P. Nation, J. Gomez, ewinston, A. Cross, J. Lishman, K. Krsulich, I. F. Sertage, S. Wood, T. Alexander, L. Capelluto, N. Kanazawa, S. de la Puente González, I. Hamamura, E. Navarro, J. Rubio, T. Imamichi, M. Tod, A. Mezzacapo, L. Bishop, S. Hu, abbycross, Zoufalc, and R. Chen, *Qiskit/qiskit-terra: Qiskit terra 0.22.3* (2022).
- [18] S. Sivarajah, S. Dilkes, A. Cowtan, W. Simmons, A. Edgington, and R. Duncan, t|ket>: a retargetable compiler for NISQ devices, *Quantum Sci. Technol.* **6**, 014003 (2020).
- [19] M. Amy and V. Gheorghiu, staq—a full-stack quantum processing toolkit, *Quantum Sci. Technol.* **5**, 034016 (2020).
- [20] B. Coecke and R. Duncan, A graphical calculus for quantum observables, Preprint (2007).
- [21] R. Duncan, A. Kissinger, S. Perdrix, and J. Van De Wetering, Graph-theoretic simplification of quantum circuits with the ZX-calculus, *Quantum* **4**, 279 (2020).
- [22] A. Kissinger and J. van de Wetering, Reducing the number of non-Clifford gates in quantum circuits, *Phys. Rev. A* **102**, 022406 (2020).
- [23] M. Amy, D. Maslov, M. Mosca, and M. Roetteler, A meet-in-the-middle algorithm for fast synthesis of depth-optimal quantum circuits, *IEEE Transactions on Computer-Aided Design of Integrated Circuits and Systems* **32**, 818 (2013).
- [24] M. Amy, D. Maslov, and M. Mosca, Polynomial-time  $T$ -depth optimization of Clifford+ $T$  circuits via matroid partitioning, *IEEE TCAD* **33**, 1476 (2014).
- [25] M. Amy and M. Mosca,  $T$ -count optimization and reed-muller codes, *IEEE Trans. Inf. Theory* **65**, 4771 (2019).
- [26] L. E. Heyfron and E. T. Campbell, An efficient quantum compiler that reduces  $T$  count, *Quantum Sci. Technol.* **4**, 015004 (2018).
- [27] V. Vandaele, Lower  $T$ -count with faster algorithms, *Quantum* **9**, 1860 (2025).
- [28] F. J. Ruiz, T. Laakkonen, J. Bausch, M. Balog, M. Barekatin, F. J. Heras, A. Novikov, N. Fitzpatrick, B. Romera-Paredes, J. van de Wetering, *et al.*, Quantum circuit optimization with alphasolver, *Nature Machine Intelligence* **7**, 374 (2025).
- [29] D. Gosset, V. Kliuchnikov, M. Mosca, and V. Russo, An algorithm for the  $T$ -count, arXiv preprint arXiv:1308.4134 (2013).
- [30] D. Litinski, A game of surface codes: Large-scale quantum computing with lattice surgery, *Quantum* **3**, 128 (2019).
- [31] Y. Hirano and K. Fujii, Locality-aware pauli-based computation for local magic state preparation, arXiv preprint arXiv:2504.12091 (2025).
- [32] F. Zhang and J. Chen, Optimizing  $T$  gates in clifford+ $T$  circuit as  $\pi/4$  rotations around paulis, arXiv preprint arXiv:1903.12456 (2019).
- [33] V. Vandaele, S. Perdrix, and C. Vuillot, Optimal number of parametrized rotations and hadamard gates in parametrized clifford circuits with non-repeated parameters, arXiv preprint arXiv:2407.07846 (2024).
- [34] Y. Mori, H. Hakoshima, K. Sudo, T. Mori, K. Mitarai, and K. Fujii, Quantum circuit nooptimization, *Phys. Rev. Res.* **7**, 023139 (2025).
- [35] A. Kissinger and J. van de Wetering, PyZX: Large scale automated diagrammatic reasoning, *Electron. Proc. Theor. Comput. Sci.* **318**, 229 (2020).
- [36] J. Håstad, Tensor rank is NP-complete, *Journal of algorithms* **11**, 644 (1990).
- [37] C. Gidney, Stim: a fast stabilizer circuit simulator, *Quantum* **5**, 497 (2021).
- [38] A. W. Cross, L. S. Bishop, J. A. Smolin, and J. M. Gambetta, Open quantum assembly language, arXiv preprint

- arXiv:1707.03429 (2017).
- [39] Reversible logic synthesis benchmarks page, <http://webhome.cs.uvic.ca/~dmaslov/> (2011).
- [40] R. Wille, L. Berent, T. Forster, J. Kunasaikaran, K. Mato, T. Peham, N. Quetschlich, D. Rovara, A. Sander, L. Schmid, *et al.*, The mqt handbook: A summary of design automation tools and software for quantum computing, arXiv preprint arXiv:2405.17543 (2024).
- [41] mcr, <https://github.com/yforest-osaka/mcr> (2025).
- [42] A. Peruzzo, J. McClean, P. Shadbolt, M.-H. Yung, X.-Q. Zhou, P. J. Love, A. Aspuru-Guzik, and J. L. O’Brien, A variational eigenvalue solver on a photonic quantum processor, *Nat. Commun.* **5**, 4213 (2014).
- [43] E. Farhi, J. Goldstone, and S. Gutmann, A quantum approximate optimization algorithm, arXiv preprint arXiv:1411.4028 (2014).
- [44] Y. Kim, A. Eddins, S. Anand, K. X. Wei, E. Van Den Berg, S. Rosenblatt, H. Nayfeh, Y. Wu, M. Zaletel, K. Temme, *et al.*, Evidence for the utility of quantum computing before fault tolerance, *Nature* **618**, 500 (2023).
- [45] Y. Akahoshi, K. Maruyama, H. Oshima, S. Sato, and K. Fujii, Partially fault-tolerant quantum computing architecture with error-corrected clifford gates and space-time efficient analog rotations, *PRX Quantum* **5**, 010337 (2024).
- [46] R. Toshio, Y. Akahoshi, J. Fujisaki, H. Oshima, S. Sato, and K. Fujii, Practical quantum advantage on partially fault-tolerant quantum computer, *Physical Review X* **15**, 021057 (2025).
- [47] J. van de Wetering, R. Yeung, T. Laakkonen, and A. Kissinger, Optimal compilation of parametrised quantum circuits, *Quantum* **9**, 1828 (2025).
- [48] Y. Nakano, H. Hakoshima, K. Mitarai, and K. Fujii, Markov-chain monte carlo method enhanced by a quantum alternating operator ansatz, *Phys. Rev. Res.* **6**, 033105 (2024).
- [49] D. Gottesman and I. L. Chuang, Demonstrating the viability of universal quantum computation using teleportation and single-qubit operations, *Nature* **402**, 390 (1999).
- [50] J. T. Anderson, On groups in the qubit clifford hierarchy, *Quantum* **8**, 1370 (2024).
- [51] J. Håstad, Tensor rank is NP-complete, *Journal of algorithms* **11**, 644 (1990).
- [52] C. Kiumi and B. Koczor, TE-PAI: exact time evolution by sampling random circuits, arXiv preprint arXiv:2410.16850 (2024).